

Published in final edited form as:

J Neurooncol. 2010 February ; 96(3): 337–347. doi:10.1007/s11060-009-9972-7.

Directed evolution of adeno-associated virus for glioma cell transduction

Casey A. Maguire¹, Davide Gianni^{1,2}, Dimphna H. Meijer³, Lev A. Shaket¹, Hiroaki Wakimoto⁴, Samuel D. Rabkin⁴, Guangping Gao⁵, and Miguel Sena-Esteves^{1,#}

¹ Department of Neurology, Massachusetts General Hospital, and Neuroscience Program, Harvard Medical School, Boston, Massachusetts, USA ² Imperial College, National Heart and Lung Institute, Imperial College, London, UK ³ Department of Neuroscience and Pharmacology, Rudolf Magnus Institute of Neuroscience, UMC Utrecht, Utrecht, the Netherlands ⁴ Department of Neurosurgery, Massachusetts General Hospital, Boston, Massachusetts, USA ⁵ University of Massachusetts Medical School, and Gene Therapy Center, Worcester, Massachusetts, USA

Abstract

Glioblastoma multiforme (GBM) is a serious form of brain cancer for which there is currently no effective treatment. Alternative strategies such as adeno-associated virus (AAV) vector mediated-genetic modification of brain tumor cells with genes encoding anti-tumor proteins have shown promising results in preclinical models of GBM, although the transduction efficiency of these tumors is often low. As higher transduction efficiency of tumor cells should lead to enhanced therapeutic efficacy, a means to rapidly engineer AAV vectors with improved transduction efficiency for individual tumors is an attractive strategy. Here we tested the possibility of identifying high-efficiency AAV vectors for human U87 glioma cells by selection in culture of a newly constructed chimeric AAV capsid library generated by DNA shuffling of six different AAV *cap* genes (AAV1, AAV2, AAV5, AAVrh.8, AAV9, and AAVrh.10). After seven rounds of selection, we obtained a chimeric AAV capsid that transduces U87 cells at high efficiency (97% at a dose of 10⁴ genome copies/cell), and at low doses it was 1.45–1.6-fold better than AAV2, which proved to be the most efficient parental capsid. Interestingly, the new AAV capsid displayed robust gene delivery properties to all glioma cells tested (including primary glioma cells) with relative fluorescence indices ranging from 1- to 14-fold higher than AAV2. The selected vector should be useful for *in vitro* glioma research when efficient transduction of several cell lines is required, and provides proof-of-concept that an AAV library can be used to generate AAV vectors with enhanced transduction efficiency of glioma cells.

Keywords

adeno-associated virus (AAV); library; brain tumor; glioblastoma; gene therapy; gene transfer

Introduction

Glioblastoma multiforme (GBM) is the highest grade primary glioma (grade IV) with a median survival time of approximately 12 months [1]. This poor survival rate is due to the inability of

Correspondence to: Miguel Sena-Esteves.

#Current address: Department of Neurology and Gene Therapy Center, University of Massachusetts Medical School, 381 Plantation Street, Suite 250, Worcester, MA 01605. Tel: (508) 856-4412; Fax: (508) 856-1552; Miguel.Esteves@umassmed.edu.

current therapies (e.g. surgery, chemotherapy, radiation) to completely remove highly invasive tumor cells, resulting in the eventual regrowth of secondary tumors near the original resection cavity [2,3]. Thus, current research for GBM therapy is focused on the elimination of these residual, post-resection tumor cells. Adeno-associated virus (AAV) vector-mediated gene delivery for brain tumor therapy using transgenes encoding anti-tumor proteins has shown promising results in experimental GBM models [4,5]. Unfortunately, transduction of experimental glioma tumors after intracranial injection with the most widely utilized AAV vector serotype 2 (AAV2) is relatively inefficient, although alternative AAV serotypes show some improvement [6,7]. In addition, the high heterogeneity of GBM tumors both among patients and within a given tumor confounds the identification of a single, highly efficient AAV serotype. This is evident in experimental glioma cell transduction experiments, where AAV2 has a different tropism depending on the glioma cell line or patient glioma isolate [8] [9,10].

Genetic engineering of targeting ligands specific for cell surface receptors into the AAV capsid has resulted in the creation of vectors with enhanced transduction properties for specific cell types [11–14]. However, not all ligands allow for capsid assembly and/or infection when placed into the structural constraints of the capsid [15,16]. Furthermore, binding to cell surface receptors is only one of many steps involved in efficient transduction by AAV vectors [17, 18]. Recently, directed molecular evolution has been used to select for AAV capsids with enhanced transductional properties for target cells [19–23]. This approach is based on performing multiple rounds of selection with libraries of AAV capsids generated by DNA shuffling of a single serotype or multiple serotypes to identify capsids with specific properties. The advantage of the DNA shuffled library-based approach, as compared to other commonly used methods of AAV capsid modification, is that detailed knowledge of capsid structure (only known for a handful of serotypes), and structural effects of targeting ligand insertion are not necessary [24,25]. The *in vitro* or *in vivo* selection process imposed upon a DNA-shuffled vector library leads to the isolation of functional vectors capable of transducing a particular cell type/organ, obviating the arduous task of testing individual capsid modifications.

In this study we developed a new AAV library generated by DNA shuffling of *cap* genes from AAV1, 2, 5, rh8, 9, and rh10, and tested whether multiple rounds of selection in cultured human U87 glioma cells would yield AAV capsids capable of transducing U87 and other glioma cells efficiently. After seven rounds of infection and rescue in U87 cells, we isolated a new chimeric AAV capsid that transduced these cells efficiently. Also, we show that one of the selected AAV vectors is more efficient than the most homologous parental serotype (AAV2) in transducing many other glioma cell types. These data underscore the potential of the DNA shuffling approach to select promising AAV vectors for GBM therapy.

Materials and Methods

Cells

The human glioblastoma cell line U87 was obtained from ATCC (Manassas, VA). Dog glioma J3T cells have been previously described [26]. GL261 mouse glioblastoma cells were obtained from Dr. E.A. Chiocca (Ohio State University). 293T cells were obtained from Dr. Michele P. Calos (Stanford University). All cells described above were cultured in high glucose Dulbecco's Modified Eagle's Medium (Invitrogen, Carlsbad, CA, USA) supplemented with 10% fetal bovine serum (Sigma, St. Louis, MO, USA) and 100 U/ml penicillin, 100 µg/ml streptomycin (Invitrogen) in a humidified atmosphere supplemented with 5% CO₂ at 37°C. Human tumor tissue used for culture of GBM20/3 cells was de-identified, discarded tissue obtained under the IRB Human Studies protocol 2002p-001135 of Dr. Robert Carter. Brain tumor specimens from patients diagnosed by a neuropathologist as glioblastoma multiforme were taken directly from surgery and placed in cold sterile Neurobasal media (Invitrogen). The specimens were dissociated into single cells within 1 hr from the time of surgery using a Neural

Tissue Dissociation Kit (Miltenyi Biotech, Bergisch Gladbach, Germany) and plated in DMEM 5% FBS supplemented with penicillin-streptomycin (10 IU ml^{-1} and $10 \mu\text{g ml}^{-1}$, respectively, Sigma). GBM8 cancer stem cells were isolated from a surgical specimen of glioblastoma as described [27]. Cells were grown as neurospheres in Neurobasal medium (Invitrogen) supplemented with 3mM L-Glutamine (Mediatech, Manassas, VA, USA), 1x B27 supplement (Invitrogen), 0.5x N2 supplement (Invitrogen), 2 $\mu\text{g/ml}$ heparin (Sigma), 20 ng/ml recombinant human EGF (R & D systems), 20 ng/ml recombinant human FGF2 (Peprotech, Rocky Hill, NJ, USA) and 0.5x penicillin G/streptomycin sulfate/amphotericin B complex (Mediatech).

AAV library construction and production

The *cap* genes for AAV serotypes AAV1, AAV2, AAV5, AAVrh.8, AAV9, and AAVrh.10 were PCR amplified with extensor Hi-Fidelity PCR Enzyme (Thermo Fisher Scientific, Waltham, MA). The *cap* gene PCR product (which also contains part of the AAV2 *rep* gene) was pooled (2 μg total DNA) and digested with 0.015 U Dnase I (New England Biolabs, Ipswich, MA) for 10 min at RT in a the reaction which was terminated using EDTA and heating for 15 min at 75°C. A gel slice containing fragments between ~300 bp–1500bp was excised with a scalpel. Subsequently, the gel slice was placed in 3,500 MWCO dialysis tubing (Fisher Scientific, Pittsburgh, PA) and the DNA was eluted into TBE by electrophoresing for 15 min at 120V. The DNA was then ethanol precipitated, resuspended in nuclease-free water and chimeric capsid genes were assembled from the digested pool of DNA by first performing a PCR without primers (thermal cycler conditions: 1cycle, 94°C 5 min; 45 cycles of 94°C 30s, 60°C 30s, 72°C 30s) and then using 1 μl of template from this PCR to perform a second PCR using a primer set (forward: 5' AAGCTTCGATCAACTACGCAG 3', reverse: 5' TATTCTAGAGCATGGAACTAGATAAG 3') which binds to a conserved region of the full length PCR product and contains HindIII and Xba I restriction sites (thermal cycler conditions: 1 cycle of 94°C 2 min; 25 cycles of 94°C 30s, 50°C 30s, 72°C 2.5 min; 1 cycle of 72°C for 7 min.) The ~2.6kbp PCR product was gel extracted (Qiagen, Valencia, CA) and digested overnight with HindIII and XbaI (both from New England Biolabs). The digested fragment was ligated with similarly digested AAV2 genome plasmid psub201 (kindly provided by Dr. Weidong Xiao, The Children's Hospital of Philadelphia), at a 3:1 insert to vector molar ratio resulting in the in-frame insertion of a pool of chimeric *cap* genes [28]. A total of 8 ligations were performed, transformed into DH10B cells (Invitrogen), and pooled for large scale DNA purification. A small volume from each transformation was plated and the total diversity of the library was determined to be 8.9×10^5 bacterial transformants.

The AAV library was produced by transient transfection of 293T cells in 15 cm plates (Corning, Corning, NY, USA) using the calcium phosphate precipitation method with the following plasmids (per plate): 4 ng psub201-AAV-Library plasmid, 25 μg of adenovirus helper plasmid Fd6 [29], and 25 μg of salmon sperm carrier DNA (Invitrogen). The small amount of library plasmid was chosen in order to ensure that only 1 plasmid was delivered to each cell so that the capsid proteins of each virion were directly linked to the DNA sequence packaged within as previously described [19]. Seventy-two hours post-transfection cells were harvested and virus purified by iodixanol gradient centrifugation followed by de-salting and concentration using Millipore Amicon Ultra centrifugal devices (Billerica, MA, USA) as described [29]. The vector titer (in genome copies/ml [gc/ml]) was determined using a quantitative TaqMan PCR assay using TaqMan® Fast Universal PCR Master Mix (Applied Biosystems, Foster City, CA, USA), a TaqMan probe (Applied Biosystems) which specifically binds to a conserved region of the AAV *rep* gene (5'CGCCGTGATTGACGGAAC3'), and two flanking primers, Rep For (5'ACCTCCAACCAACATGT3') and Rep Rev (5'CTGCTGGTGTTCGAAGGT3') [30]. A standard curve was prepared using serial dilutions of psub201 plasmid of a known molar concentration. The quantitative PCR was performed in an Applied Biosystems 7500

Thermal cycler using the following conditions: 1 cycle, 94°C 30s; 40 cycles 94°C 3s, 60°C 30s.

***In vitro* selection**

Twenty-four hours prior to infection, U87 cells were plated at a density of 100,000 cells/well in a 24 well plate and incubated at 37°C. The following day, 10^3 gc/cell was applied to the cells in 300 µl of serum-free media for 2 h at 37°C. Next, uninternalized vector was removed by rinsing the cells twice in serum-free media after which wild type Adenovirus serotype 5 (Ad5) (ATCC) was added at a multiplicity of infection of 100 (in 300 µl complete media) to rescue internalized AAV genomes. Forty-eight hours post-Ad5 infection, cells and medium were harvested and subjected to 3 freeze/thaw cycles in a dry ice/ethanol bath and 37°C water bath. Ad5 present in cell lysates was heat-inactivated by incubation at 56°C for 30 min. Cell debris was pelleted by centrifugation in a microcentrifuge for 5 min at $5,000 \times g$, and the supernatant harvested for titration and use for the second round of selection. Titration for total recovered AAV genomes (gc) in crude cell lysate was performed as previously described [31]. Briefly 5 µl of crude lysate was incubated with 4.5 µg DNaseI (New England Biolabs) in 50 µl of 1x buffer for 30 min at 37°C. DNaseI was inactivated at 75°C for 25 min along with the addition of 2 mM EDTA. The lysate was further treated with 5 µg of Proteinase K (Qiagen) at 37°C for 30 min followed by inactivation at 95°C for 20 min. Two µl of a 1:10 dilution of the treated lysate was used for the quantitative *rep* PCR described above. Two more rounds were performed using the appropriate volume of lysate from the previous round to give 10^3 gc/cell. After the third round the full-length capsid gene was amplified from 2 µl of crude lysate treated as above using Phusion™ High-Fidelity DNA Polymerase (New England Biolabs). Thermal cycler conditions were as follows: 1cycle, 98°C-30s; 35 cycles, 98°C-10s, 50°C-10s, 72°C-1.5 min; 1cycle, 72°C-7 min. The PCR product was gel extracted, digested with HindIII and XbaI, and ligated with similarly digested pH22 vector, which provides AAV2 Rep and Cap in trans [32]. Digestion with HindIII and XbaI replaced the AAV2 cap gene (and part of the *rep* gene) with the selected capsid gene(s). After transformation of the vector into DH10B bacterial cells, a single clone was picked and a large-scale preparation of DNA made. After DNA sequencing of the U87-selected capsid gene, a purified vector comprised of an ITR-flanked GFP expression cassette packaged within the chimeric capsid was produced as previously described [33]. A similar strategy was used for isolation of the round 7 selected vectors except that starting with the round 3 lysate, each subsequent round used 1 µl of a 1:100 dilution of lysate from the prior round. Purifications of AAV2-GFP, AAV-U87R7-C5 and some other vectors used in this study were carried out by either iodixanol or cesium chloride gradient sedimentation method. Vectors containing the capsids of parental serotypes with the Fluc cassette were also produced as described [33].

***In vitro* transduction assays**

Luciferase reporter assay—U87 cells were transduced with 5×10^3 gc/cell of the six parental AAV vectors encoding firefly luciferase (Fluc). The genome in these vectors was AAV-CBA-Fluc-W derived from AAV-CBA-GFP-W by replacing the GFP cassette with Fluc cDNA (Promega, Madison, WI, USA)[29]. Seventy-two hours post-transduction cell lysates were prepared, and a luciferase assay was performed using a Luciferase Assay System kit (Promega) and reading luciferase levels with a microtiter plate luminometer (Dynex Technologies, Chantilly, VA, USA). Luciferase levels (expressed as Relative Light Units) were normalized to total protein content of each sample using a Bradford assay (Bio-Rad, Hercules, CA, USA).

GFP reporter assay—The various cell lines or primary cell types indicated in the figure legends were plated and transduced (dose indicated in figure legend) the following day with the indicated AAV vector encoding GFP. Forty-eight or seventy-two hours later, cells were

analyzed for GFP expression using a fluorescence microscope. Subsequently, the percentage of GFP positive cells was determined by flow cytometry using a FACSCalibur flow cytometer (BD, Franklin Lakes, NJ). For expression kinetic analysis, cells were harvested at 24, 48, and 72 hours post-transduction for flow cytometric analysis. Percentages of GFP positive cells and mean fluorescence intensity were determined using CellQuest software (BD Biosciences, San Jose, CA).

Heparin blocking assay— 10^9 gc of the indicated AAV vector encoding GFP was incubated with 100 μ g/ml of heparin (Stem Cell Technologies, Vancouver, BC, Canada) for 30 min at room temperature before adding the mixture to 10^5 U87 cells for 1h at 37°C. Cells were then rinsed and incubated for 72 hours before analyzing cells for GFP expression using a FACSCalibur flow cytometer.

Statistics

Data presented provides the mean \pm 1 standard deviation. For some figures, group comparisons were computed by an unpaired Student's t-test using GraphPad PRISM software (version 5.0; San Diego, CA).

Results

Construction and sequence analysis of a novel DNA-shuffled AAV library

The *cap* genes from six AAV serotype/variants (AAV1, AAV2, AAV5, AAVrh.8, AAV9, and AAVrh.10) were PCR-amplified from plasmids using specific primers (see Methods). The *cap* gene DNAs were then mixed in equal ratios and subjected to DNA shuffling, as previously described using error-prone PCR, to generate a pool of AAV genome plasmids encoding chimeric AAV capsids with a total diversity of 8.9×10^5 bacterial transformants [34]. This pool of AAV genome plasmids was used to prepare a stock of purified AAV virions (AAV library) with a titer of 5.3×10^{11} genome copies (gc)/ml. To confirm the chimeric nature and diversity of packaged AAV genomes, we PCR-amplified *cap* genes (~ 2.2 kbp) in the AAV library and sequenced 10 individual clones. The complete nucleotide sequence was converted into deduced amino acid sequence and aligned using Vector NTI AlignX (Supplementary Figure 1). This analysis showed that all 10 clones encoded chimeric capsid genes comprised of two or more AAV serotypes, and that each clone carried unique amino acid changes at different positions (introduced by error-prone PCR). Although none of the 10 clones carried sequences unique to AAV5 or AAV9, PCR analysis of AAV library DNA using primers specific for a divergent region on each of those two *cap* genes, showed that AAV5 and AAV9 *cap* sequences are present in the library (Supplementary Figure 2) [21]. Importantly, no wild type AAV2 (used for the library backbone) was ever detected by sequencing. Thus our AAV capsid library encodes chimeric capsids derived from all six parental AAV *cap* genes as well as novel sequence variations within them.

Selection of an AAV library in cell culture yields a vector which efficiently transduces U87 glioma cells

Having successfully created a chimeric AAV library, we assessed whether repeated rounds of selection by infection of cultured cells would result in the selection of vectors with enhanced gene delivery properties, as compared to AAV vectors based on the parental capsids. The unselected AAV library was added to U87 glioma cells at a dose of 10^3 gc/cell and incubated for 2 hours at 37°C. After thorough rinsing to remove unbound/uninternalized virus, wild type Adenovirus serotype 5 (Ad5) was added at a dose of 100 plaque forming units (PFU)/cell to rescue AAV genomes which had successfully infected U87 cells. Forty-eight hours post-Ad5 infection, the cells and media were harvested, subjected to freeze/thaw cycles, and the titer of AAV genomes in the lysate determined by quantitative PCR. The crude lysate from round 1

was used to again infect U87 cells at a dose of 10^3 gc/cell. An identical process of infection, rescue and titer determination was performed for the second and third rounds of selection. Between round 1 and 2, the total recovered genomes increased from 9.29×10^8 gc to 1.45×10^{11} gc, respectively, a 156-fold enrichment in virus recovery (Figure 1A). The total recovered genomes reached a plateau by round two as there was no further increase in the third round. Based on the overall increase in recovered virus between round 1 and 3, the full length *cap* gene was PCR amplified from virus isolated from round 3 using *cap*-flanking primers and then the digested PCR product was cloned into pH22, which is an AAV-helper plasmid carrying AAV2 *rep* and *cap* genes (AAV2 *cap* gene is replaced during cloning) in the absence of ITR elements. One clone from round 3 harboring the U87-selected *cap* gene (termed AAV-U87R3) was chosen at random and sequenced. Analysis of the nucleotide sequence of AAV-U87R3 revealed that it was a chimeric capsid composed of AAV1, AAVrh.8, AAVrh.10, and AAV2 sequences. Its deduced amino acid sequence was most homologous to AAV2 (Figure 1B). Interestingly the motifs involved in heparan sulfate binding (including the one at 585–588, RGNR) were intact in this clone, suggesting their importance for cell binding [35]. Additional point mutations (presumably caused by the error-prone PCR process during DNA shuffling) were observed in both AAV1/rh10 and AAV2 sequences (N14D, N496Y, K527R, H627Y). Next, AAV-U87R3 was used to produce a recombinant AAV vector encoding GFP for transduction analysis of U87 cells. Only low levels of transduction were observed by fluorescence microscopy 48h after adding this vector to U87 cells (data not shown). We next performed additional rounds of selection to ascertain if more efficient clones could be isolated. As a plateau in genome recovery was observed after round 2 of selection using a fixed 10^3 gc/cell input/round, for the fourth round of selection 50 gc/cell was used to attempt to increase the stringency of selection. For rounds 5–7 the same magnitude of dilution used in round 4 was performed, although the precise vector input was not calculated. After 7 rounds of infection/rescue we amplified and cloned AAV *cap* genes for sequence analysis. The 5' and 3' ends of 10 individual *cap* clones were sequenced. Alignment of the 5' sequences segregated the clones into 2 groups (5 clones in each), one comprised of sequences unique to AAV1, AAV2, AAVrh.8 and AAVrh.10, and the other with sequences unique to AAV1, AAVrh.8, and AAVrh.10 (data not shown). The 3' ends of all 10 clones were homologous to AAV2 with various point mutations observed. Based on this analysis, one representative capsid clone from each of the two 5' aligning groups (termed AAV-U87R7-C1 and AAV-U87R7-C5) was chosen for full *cap* gene sequence analysis. A schematic of the AAV variant-specific amino acid composition of these clones is shown in Figure 1B. These clones also contained point mutations in the homologous capsid sequences, as indicated. Interestingly, AAV-U87R3 and AAV-U87R7-C1 differed by only 3 amino acids and AAV-U87R7-C5 shared a mutation, H627Y in the AAV2 sequence with AAV-U87R3.

Next, clones AAV-U87R7-C1, and AAV-U87R7-C5 were used to produce small-scale iodixanol purified preparations of recombinant AAV vectors encoding GFP for transduction analysis of U87 cells. Since AAV2 proved to be the most efficient vector to transduce U87 cells in culture (Figure 2), we used AAV2-GFP vector as a reference to gauge the efficiency of all new AAV vectors. U87 cells were incubated with AAV2-GFP, AAV-U87R7-C1-GFP, and AAV-U87R7-C5-GFP vectors at a dose of 10^4 gc/cell, and at 48 h we analyzed GFP expression by fluorescence microscopy. Surprisingly we did not find any GFP-positive U87 cells for AAV-U87R7-C1-GFP vector (data not shown). Additional transduction experiments with this vector in the presence of Ad5 helper showed the same result (data not shown) and thus this vector was excluded from further analysis. In contrast, efficient transduction was observed for AAV-U87R7-C5-GFP (data not shown). For subsequent studies we used AAV2-GFP and AAV-U87R7-C5-GFP vectors purified by cesium chloride gradient centrifugation to eliminate empty capsids from the preparations as it has been reported that iodixanol gradient purification does not consistently remove all empty capsids [36]. Analysis of the cesium chloride gradient-purified vectors by silver staining revealed highly purified preparations

(Figure 3A). Interestingly the VP2 protein of AAV-U87R7-C5-GFP migrated at a higher molecular weight than that of AAV2 most likely due to differences in amino acid sequence between the two vectors (Figure 3A). AAV2-GFP and AAV-U87R7-C5-GFP vectors were used to transduce U87 cells at doses of 10^4 , 10^3 , 10^2 , and 50 gc/cell, and 72 h later we analyzed transduction efficiency by fluorescence microscopy (Figure 3B) and flow cytometry. AAV2-GFP and AAV-U87R7-C5-GFP vectors transduced U87 cells efficiently at 10^4 gc/cell, with a mean of 97% GFP positive cells for both vectors (Figure 3C). At 10^3 gc/cell, AAV-U87R7-C5-GFP transduced U87 cells 1.1-fold better than AAV2-GFP ($P=0.009$) in terms of percentage of GFP positive cells (Figure 3C). AAV-U87R7-C5-GFP displayed an even greater increase compared to AAV2-GFP in the percentage of GFP positive cells at 10^2 gc/cell (1.6-fold, $P<0.0001$) and 50 gc/cell (1.45-fold, $P<0.0001$) (Figure 3C). No significant difference between AAV2-GFP and AAV-U87R7-C5-GFP was detected in mean fluorescence intensity (MFI) at any dose, with the exception of 10^2 gc/cell, where there was a 1.3-fold higher ($P=0.01$) MFI for AAV2-GFP compared to AAV-U87R7-C5-GFP (Figure 3D). A time course (24–72h) analysis of transgene expression in U87 cells mediated by either AAV2-GFP or AAV-U87R7-C5-GFP revealed no significant differences in the kinetics of expression between the two vectors (Figure 4A, B). Next we analyzed whether entry of AAV-U87R7-C5-GFP into U87 cells was dependent on heparan sulfate as the amino acids (RGNR) implicated in this interaction [35] were intact in this clone. As expected, incubation of AAV2-GFP or AAV-U87R7-C5-GFP in the presence of heparin greatly reduced transduction efficiency, with a decrease in both the percentage of GFP positive cells and MFI (Figure 4C).

Transduction efficiency of newly selected chimeric capsid clone on several glioma cell types

Since the N-terminus of the AAV-U87R7-C5-GFP capsid is derived from parental AAV capsids other than AAV2, we speculated that an AAV vector carrying this chimeric capsid could have different transduction properties in other glioma cells compared to an AAV2 vector. To assess this possibility, we tested the transduction efficiency of AAV2-GFP, and AAV-U87R7-C5-GFP (at 10^4 gc/cell) on a panel of cells consisting of J3T dog astrocytoma cells, GL261 mouse glioma cells, and primary human glioblastoma cells (GBM8 brain cancer stem cells and GBM 20/3). Also we compared the transduction efficiency on a non-glioma cell line, HEK293T. Interestingly, AAV-U87R7-C5-GFP vector displayed a robust transductional profile on the majority of cells tested (Figure 5A–E). Moreover, the transduction efficiency measured by the relative fluorescence index (calculated for each sample by multiplying the percentage of GFP positive cells by the mean fluorescence intensity) was significantly better than AAV2-GFP on all cells tested with the exception of GBM 20/3 primary human glioblastoma cells (Figure 5F). The most striking difference between the two vectors was observed on mouse GL261 glioblastoma cells where AAV-U87R7-C5-GFP transduced 91.5% of cells compared to only 26.9% of cells for AAV2-GFP (Figure 5B). Furthermore, there was a ~4-fold (from 66.7 to 216.3) increase in MFI when using AAV-U87R7-C5-GFP suggesting that several more vectors were successfully transducing individual cells compared to AAV2. Accordingly, the relative fluorescence index of AAV-U87R7-C5-GFP in GL261 cells was 14-fold higher than AAV2-GFP (Figure 5F). Interestingly, cell attachment was still dependent on heparan sulfate, as pre-incubating AAV-U87R7-C5-GFP with heparin, greatly reduced transduction efficiency (data not shown).

Discussion

Efficient transduction of brain tumor cells, and in some cases normal peritumoral cells, is believed to be a prerequisite for obtaining a robust anti-tumor effect when using viral vectors for GBM therapy. In this study we constructed a new AAV capsid library and performed multiple rounds of selection in cell culture to identify new AAV capsids capable of transducing human U87 cells effectively. This strategy yielded a new chimeric AAV capsid capable of

efficient transduction of U87 and other glioma cell types. In U87 cells, the new AAV capsid was comparable to the most efficient parental capsid (AAV2) at a vector dose of 10^4 gc/ml, and 1.45-fold better at lower doses. In primary glioma cells the transduction efficiency was comparable to that of AAV2, while in dog J3T and mouse GL261 glioma cell lines there was a considerable increase in transduction efficiency (26.9 to 91.5% in the latter cell line).

AAV2 has been shown to transduce glioma cell lines more efficiently than AAV1, AAV4 and AAV5 [6,10]. Here we found that AAV2 is more efficient than AAV1, AAV5, AAVrh.8, AAV9 and AAVrh.10 for transduction of U87 glioma cells in culture (Figure 2). Thus it is not surprising that the clones isolated from a directed-evolution approach had the highest homology with AAV2 (>95%). Since AAV2 transduces U87 cells efficiently (~100% of cells transduced at 10^4 gc/cell), a DNA shuffled library created by error-prone PCR based on AAV2 may be one way to increase transduction of this particular cell type by an even greater fold [19]. Obtaining new chimeric AAV capsids much better than all parental AAV variants may be most effective on cell types highly resistant to transduction [22], such as GBM8 cancer stem cells (Figure 5). It may also be worthwhile to construct highly diverse AAV libraries which consist of DNA shuffled, multi-serotype capsids pooled with AAV capsids of individual serotypes generated by error-prone PCR. Furthermore, the greatest advantage with chimeric AAV libraries appears to be the ability to perform more complex selections in which efficient transduction is coupled to another property (e.g. ability to avoid AAV2-specific neutralizing antibodies, or the ability to bypass non-target tissue after intravenous delivery) [20].

The round 7-selected clone AAV-U87R7-C5 showed transduction efficiency in U87 cells which rivaled, and at some doses, was superior to the most efficient and most homologous vector, AAV2. Interestingly, we found that the selected capsid had enhanced transduction efficiency on many glioma cells (GL261, J3T, and primary GBM-8 stem cells) compared to AAV2 (Figure 5). It is quite interesting that the novel vector displayed such a high degree of homology to AAV2 (>95%) and while it yielded similar transduction efficiency as AAV2 on the target cells (U87), in GL261 cells the new vector was 14-fold more efficient (as measured by the relative fluorescence index) than AAV2. This result (albeit a serendipitous finding) underscores the ability of directed evolution approaches to yield vectors with new and useful properties. These results also indicate that the newly selected capsid has unique properties in comparison to its most homologous AAV serotype (AAV2). It is unclear at this time at what step(s) in the pathway of gene delivery this capsid differs from AAV2 but based on heparin blocking assays it appears to be post-attachment. Discerning how such small contributions from the other AAV variants yielded such a robust transduction efficiency on some of the cell lines tested may provide important clues on how to design vectors with motifs from alternative serotypes/variants which can enhance transduction of certain resistant cell types.

We also observed that one of the round 7-selected capsids (AAV-U87R7-C1) did not show transduction of U87 cells at the dose tested. Although we used a PCR enzyme with proof-reading activity to amplify the 2.2 kbp *cap* gene, one possibility for the apparently non-functional clone is that the PCR-based strategy utilized to recover capsid genes after selection may have introduced further mutations which altered the ability to deliver transgenes to the target cell type. This is an important caveat to consider when performing these selections.

Recently, Ward et al. isolated an AAV vector from a DNA-shuffled library evolved on Hep G2 cells which yielded a slight increase in transduction efficiency compared to AAV2 [37]. The authors found no such enhancement on 293T or HepB3 cells. In contrast, the round 7 clone selected on U87 in this study displayed a broad tropism for multiple cell lines and primary cells. Thus it appears that if a vector with either expanded or restricted tropism is preferred, a more complex negative selection or multi-cell type selection should be performed to isolate an AAV capsid with the desired properties.

While we demonstrated that the round 7 *in vitro*-selected AAV clone could transduce cells in culture, selection of AAV capsids which allow more efficient transduction of glioma tumors after intracranial injection will most likely require the selection process to be performed *in vivo* due to the more complex properties of a three-dimensional solid tumor compared to cultured cells (e.g. high interstitial pressure, extracellular matrix, altered receptor profile). Further supporting this notion is the fact that the transduction efficiency of AAV serotypes on cultured glioma cells does not correlate well with their transduction efficiency of glioma tumors *in vivo* [7]. Since our AAV library was constructed in part from AAV variants that perform exceptionally well *in vivo* (i.e. AAVrh.8, AAV9, AAVrh.10), it may be well suited for such an *in vivo* selection [38–40].

In conclusion, we have shown that selection of a DNA-shuffled AAV capsid library in cultured U87 cells yielded a new chimeric AAV capsid capable of efficient gene transfer to those cells. In addition, this capsid displayed enhanced transduction of other glioma cell lines compared to the AAV2 serotype with which it shared the highest homology. This vector will be very useful for glioma research as it allows the researcher to use a single vector to obtain efficient transduction on many glioma cell types (at least the ones tested here). In the future it may be possible to use this type of chimeric capsid AAV library to select for customized vectors which can efficiently deliver transgenes encoding anti-tumor proteins to individual GBM tumors *in vivo* by performing rounds of intravenous or intratumoral injections of library with subsequent rescue of vector from tumor biopsy material. Alternatively, selections on cultured sections of tumor biopsy material may be performed *ex vivo*.

Supplementary Material

Refer to Web version on PubMed Central for supplementary material.

Acknowledgments

This work was supported by a Young Investigator Award from the Alliance for Cancer Gene Therapy (MSE), NIH T32CA073479 (CM), and NIH P50CA86355 (MSE). We would like to acknowledge Dr. Rakesh Jain and the Edwin L. Steele Laboratory at MGH for support during this study. We would like to thank the MGH Nucleic Acid Quantitation Core facility supported by NINDS grant #P30NS4577 for the use of the thermal cyclers for quantitative PCR. Drs. Johan Skog and Robert Carter for kindly providing the primary glioblastoma cells. We thank Johanna Niers for help with cell culture. We would like to thank Dr. Xandra O. Breakefield for advice and critical reading of the manuscript.

References

1. Wensch M, Minn Y, Chew T, Bondy M, Berger MS. Epidemiology of primary brain tumors: current concepts and review of the literature. *Neuro Oncol* 2002;4:278–299. [PubMed: 12356358]
2. Wallner KE, Galicich JH, Krol G, Arbit E, Malkin MG. Patterns of failure following treatment for glioblastoma multiforme and anaplastic astrocytoma. *Int J Radiat Oncol Biol Phys* 1989;16:1405–1409. [PubMed: 2542195]
3. Stewart LA. Chemotherapy in adult high-grade glioma: a systematic review and meta-analysis of individual patient data from 12 randomised trials. *Lancet* 2002;359:1011–1018. [PubMed: 11937180]
4. Yoshida J, Mizuno M, Nakahara N, Colosi P. Antitumor effect of an adeno-associated virus vector containing the human interferon-beta gene on experimental intracranial human glioma. *Jpn J Cancer Res* 2002;93:223–228. [PubMed: 11856487]
5. Mizuno M, Yoshida J, Colosi P, Kurtzman G. Adeno-associated virus vector containing the herpes simplex virus thymidine kinase gene causes complete regression of intracerebrally implanted human gliomas in mice, in conjunction with ganciclovir administration. *Jpn J Cancer Res* 1998;89:76–80. [PubMed: 9510479]
6. Huszthy PC, Svendsen A, Wilson JM, Kotin RM, Lonning PE, Bjerkvig R, Hoover F. Widespread dispersion of adeno-associated virus serotype 1 and adeno-associated virus serotype 6 vectors in the

- rat central nervous system and in human glioblastoma multiforme xenografts. *Hum Gene Ther* 2005;16:381–392. [PubMed: 15812233]
7. Harding TC, Dickinson PJ, Roberts BN, Yendluri S, Gonzalez-Edick M, Lecouteur RA, Jooss KU. Enhanced gene transfer efficiency in the murine striatum and an orthotopic glioblastoma tumor model, using AAV-7- and AAV-8-pseudotyped vectors. *Hum Gene Ther* 2006;17:807–820. [PubMed: 16942441]
 8. Reardon DA, Wen PY. Therapeutic advances in the treatment of glioblastoma: rationale and potential role of targeted agents. *Oncologist* 2006;11:152–164. [PubMed: 16476836]
 9. Wollmann G, Tattersall P, van den Pol AN. Targeting human glioblastoma cells: comparison of nine viruses with oncolytic potential. *J Virol* 2005;79:6005–6022. [PubMed: 15857987]
 10. Thorsen F, Afione S, Huszthy PC, Tysnes BB, Svendsen A, Bjerkvig R, Kotin RM, Lonning PE, Hoover F. Adeno-associated virus (AAV) serotypes 2, 4 and 5 display similar transduction profiles and penetrate solid tumor tissue in models of human glioma. *J Gene Med* 2006;8:1131–1140. [PubMed: 16810631]
 11. Grifman M, Trepel M, Speece P, Gilbert LB, Arap W, Pasqualini R, Weitzman MD. Incorporation of tumor-targeting peptides into recombinant adeno-associated virus capsids. *Mol Ther* 2001;3:964–975. [PubMed: 11407911]
 12. Girod A, Ried M, Wobus C, Lahm H, Leike K, Kleinschmidt J, Deleage G, Hallek M. Genetic capsid modifications allow efficient re-targeting of adeno-associated virus type 2. *Nat Med* 1999;5:1052–1056. [PubMed: 10470084]
 13. Buning H, Ried MU, Perabo L, Gerner FM, Huttner NA, Enssle J, Hallek M. Receptor targeting of adeno-associated virus vectors. *Gene Ther* 2003;10:1142–1151. [PubMed: 12833123]
 14. Work LM, Buning H, Hunt E, Nicklin SA, Denby L, Britton N, Leike K, Odenthal M, Drebber U, Hallek M, Baker AH. Vascular bed-targeted in vivo gene delivery using tropism-modified adeno-associated viruses. *Mol Ther* 2006;13:683–693. [PubMed: 16387552]
 15. Warrington KH Jr, Gorbatyuk OS, Harrison JK, Opie SR, Zolotukhin S, Muzyczka N. Adeno-associated virus type 2 VP2 capsid protein is nonessential and can tolerate large peptide insertions at its N terminus. *J Virol* 2004;78:6595–6609. [PubMed: 15163751]
 16. Yang Q, Mamounas M, Yu G, Kennedy S, Leaker B, Merson J, Wong-Staal F, Yu M, Barber JR. Development of novel cell surface CD34-targeted recombinant adeno-associated virus vectors for gene therapy. *Hum Gene Ther* 1998;9:1929–1937. [PubMed: 9741431]
 17. Wu Z, Asokan A, Samulski RJ. Adeno-associated virus serotypes: vector toolkit for human gene therapy. *Mol Ther* 2006;14:316–327. [PubMed: 16824801]
 18. Buning H, Perabo L, Coutelle O, Quad-Humme S, Hallek M. Recent developments in adeno-associated virus vector technology. *J Gene Med* 2008;10:717–733. [PubMed: 18452237]
 19. Maheshri N, Koerber JT, Kaspar BK, Schaffer DV. Directed evolution of adeno-associated virus yields enhanced gene delivery vectors. *Nat Biotechnol* 2006;24:198–204. [PubMed: 16429148]
 20. Grimm D, Lee JS, Wang L, Desai T, Akache B, Storm TA, Kay MA. In Vitro and In Vivo Gene Therapy Vector Evolution via Multispecies Interbreeding and Retargeting of Adeno-Associated Viruses. *J Virol* 2008;82:5887–5911. [PubMed: 18400866]
 21. Koerber JT, Jang JH, Schaffer DV. DNA shuffling of adeno-associated virus yields functionally diverse viral progeny. *Mol Ther* 2008;16:1703–1709. [PubMed: 18728640]
 22. Li W, Asokan A, Wu Z, Van Dyke T, Diprimio N, Johnson JS, Govindaswamy L, Agbandje-McKenna M, Leightle S, Eugene Redmond D Jr, McCown TJ, Petermann KB, Sharpless NE, Samulski RJ. Engineering and Selection of Shuffled AAV Genomes: A New Strategy for Producing Targeted Biological Nanoparticles. *Mol Ther* 2008;16:1252–1260. [PubMed: 18500254]
 23. Kwon I, Schaffer DV. Designer gene delivery vectors: molecular engineering and evolution of adeno-associated viral vectors for enhanced gene transfer. *Pharm Res* 2008;25:489–499. [PubMed: 17763830]
 24. Perabo L, Buning H, Kofler DM, Ried MU, Girod A, Wendtner CM, Enssle J, Hallek M. In vitro selection of viral vectors with modified tropism: the adeno-associated virus display. *Mol Ther* 2003;8:151–157. [PubMed: 12842438]

25. White SJ, Nicklin SA, Buning H, Brosnan MJ, Leike K, Papadakis ED, Hallek M, Baker AH. Targeted gene delivery to vascular tissue in vivo by tropism-modified adeno-associated virus vectors. *Circulation* 2004;109:513–519. [PubMed: 14732747]
26. Sena-Esteves M, Hampl JA, Camp SM, Breakefield XO. Generation of stable retrovirus packaging cell lines after transduction with herpes simplex virus hybrid amplicon vectors. *J Gene Med* 2002;4:229–239. [PubMed: 12112640]
27. Wakimoto H, Kesari S, Farrell CJ, Curry WT Jr, Zaupa C, Aghi M, Kuroda T, Stemmer-Rachamimov A, Shah K, Liu TC, Jeyaretna DS, Debasitis J, Pruszk J, Martuza RL, Rabkin SD. Human glioblastoma-derived cancer stem cells: Establishment of invasive glioma models and treatment with oncolytic herpes simplex virus vectors. *Cancer Res* 2009;69:3472–3481. [PubMed: 19351838]
28. Walsh CE, Liu JM, Xiao X, Young NS, Nienhuis AW, Samulski RJ. Regulated high level expression of a human gamma-globin gene introduced into erythroid cells by an adeno-associated virus vector. *Proc Natl Acad Sci U S A* 1992;89:7257–7261. [PubMed: 1323131]
29. Broekman ML, Comer LA, Hyman BT, Sena-Esteves M. Adeno-associated virus vectors serotyped with AAV8 capsid are more efficient than AAV-1 or -2 serotypes for widespread gene delivery to the neonatal mouse brain. *Neuroscience* 2006;138:501–510. [PubMed: 16414198]
30. Gao G, Alvira MR, Somanathan S, Lu Y, Vandenberghe LH, Rux JJ, Calcedo R, Sanmiguel J, Abbas Z, Wilson JM. Adeno-associated viruses undergo substantial evolution in primates during natural infections. *Proc Natl Acad Sci U S A* 2003;100:6081–6086. [PubMed: 12716974]
31. Mayginnnes JP, Reed SE, Berg HG, Staley EM, Pintel DJ, Tullis GE. Quantitation of encapsidated recombinant adeno-associated virus DNA in crude cell lysates and tissue culture medium by quantitative, real-time PCR. *J Virol Methods* 2006;137:193–204. [PubMed: 16860883]
32. Hauck B, Xiao W. Characterization of tissue tropism determinants of adeno-associated virus type 1. *J Virol* 2003;77:2768–2774. [PubMed: 12552020]
33. Maguire CA, Meijer DH, Leroy SG, Tierney LA, Broekman ML, Costa FF, Breakefield XO, Stemmer-Rachamimov A, Sena-Esteves M. Preventing Growth of Brain Tumors by Creating a Zone of Resistance. *Mol Ther* 2008;16:1695–1702. [PubMed: 18714312]
34. Stemmer WP. Rapid evolution of a protein in vitro by DNA shuffling. *Nature* 1994;370:389–391. [PubMed: 8047147]
35. Kern A, Schmidt K, Leder C, Muller OJ, Wobus CE, Bettinger K, Von der Lieth CW, King JA, Kleinschmidt JA. Identification of a heparin-binding motif on adeno-associated virus type 2 capsids. *J Virol* 2003;77:11072–11081. [PubMed: 14512555]
36. Wu P, Xiao W, Conlon T, Hughes J, Agbandje-McKenna M, Ferkol T, Flotte T, Muzyczka N. Mutational analysis of the adeno-associated virus type 2 (AAV2) capsid gene and construction of AAV2 vectors with altered tropism. *J Virol* 2000;74:8635–8647. [PubMed: 10954565]
37. Ward P, Walsh CE. Chimeric AAV Cap sequences alter gene transduction. *Virology* 2009;386:237–248. [PubMed: 19232422]
38. Cearley CN, Vandenberghe LH, Parente MK, Carnish ER, Wilson JM, Wolfe JH. Expanded repertoire of AAV vector serotypes mediate unique patterns of transduction in mouse brain. *Mol Ther* 2008;16:1710–1718. [PubMed: 18714307]
39. Cearley CN, Wolfe JH. Transduction characteristics of adeno-associated virus vectors expressing cap serotypes 7, 8, 9, and Rh10 in the mouse brain. *Mol Ther* 2006;13:528–537. [PubMed: 16413228]
40. Sondhi D, Hackett NR, Peterson DA, Stratton J, Baad M, Travis KM, Wilson JM, Crystal RG. Enhanced survival of the LINCL mouse following CLN2 gene transfer using the rh.10 rhesus macaque-derived adeno-associated virus vector. *Mol Ther* 2007;15:481–491. [PubMed: 17180118]

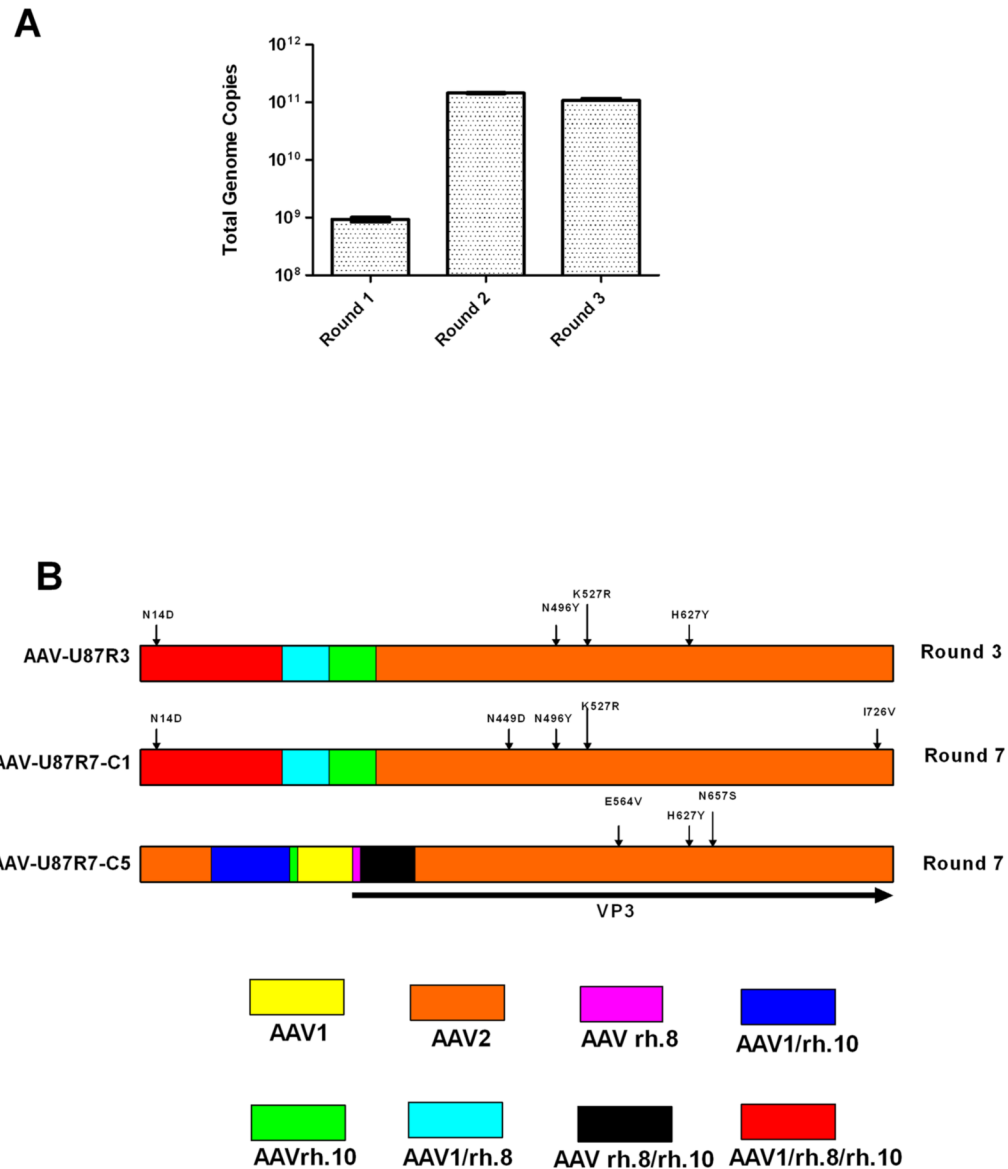


Figure 1. Selection of novel AAV capsids for efficient transduction of U87 glioma cells
(A) U87 cells were infected with 10^3 gc/cell of unselected AAV library, followed 2 hours later by infection with Adenovirus-5 at MOI of 100 to rescue AAV genomes from transduced cells. Two days later crude cell lysates were prepared, titrated for AAV genomes and used for subsequent rounds of selection. Two more rounds were performed. The total number of rescued vector genomes was determined by quantitative PCR after each round. Error bars indicate the standard deviation from the mean **(B)** AAV amino acid composition of selected capsid clones after 3 and 7 rounds of selection. Round 7 clones segregated into two families of homology represented by clones AAV-U87R7-C1 and AAV-U87R7-C5. The schematic shows the homology of each region of the capsid. Point mutations presumably introduced during PCR amplification are indicated by arrows.

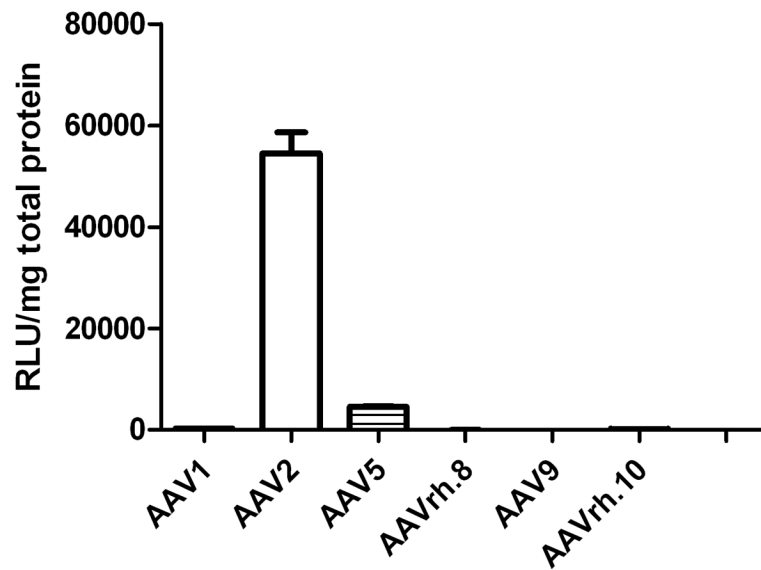


Figure 2. Transduction properties of parental serotypes on U87 cells

U87 cells were transduced with the six parental serotypes (5×10^3 gc/cell) used to create the library to determine the most efficient vector on these cells. Sixty hours post-transduction cells were lysed and a luciferase assay performed. Error bars indicate the standard deviation from the mean

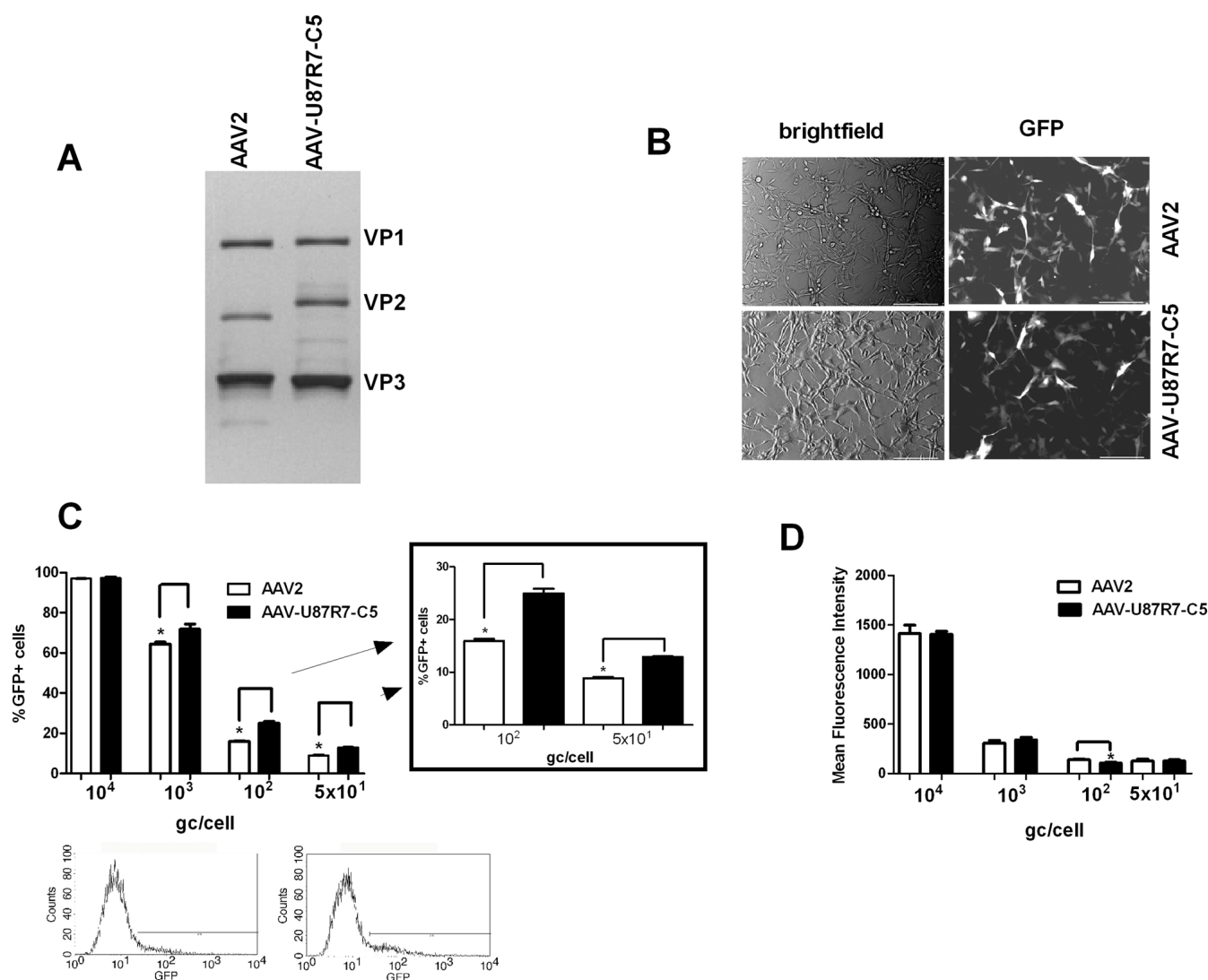


Figure 3. Round 7-selected clone transduces U87 cells efficiently

(A) Silver stain of cesium chloride gradient-purified AAV-GFP vectors. (B) Bright field and fluorescence micrographs of AAV2 and AAV-U87R7-C5-transduced U87 cells. Left panels depict bright field images and right panels show fluorescence. U87 cells were transduced with 10^4 gc/cell of either vector and seventy-two hours later, cells were analyzed for GFP expression. Scale bars, 200µm. (C) Percentages of GFP positive cells determined by flow cytometric analysis of transduced cells. Boxed graph depicts a magnification of the lower dose data. Flow histograms depict GFP expression in representative samples of U87 cells transduced with 50 gc/cell of either AAV2-GFP (left) or AAV-U87R7-C5-GFP (right). M1 is the region of GFP positive cells which was positioned using a non-transduced sample to include a background of 1% of cells. (D) Mean fluorescence intensity (MFI) of GFP positive cells determined by flow cytometric analysis of transduced cells. Error bars indicate the standard deviation from the mean. * indicates $P < 0.05$.

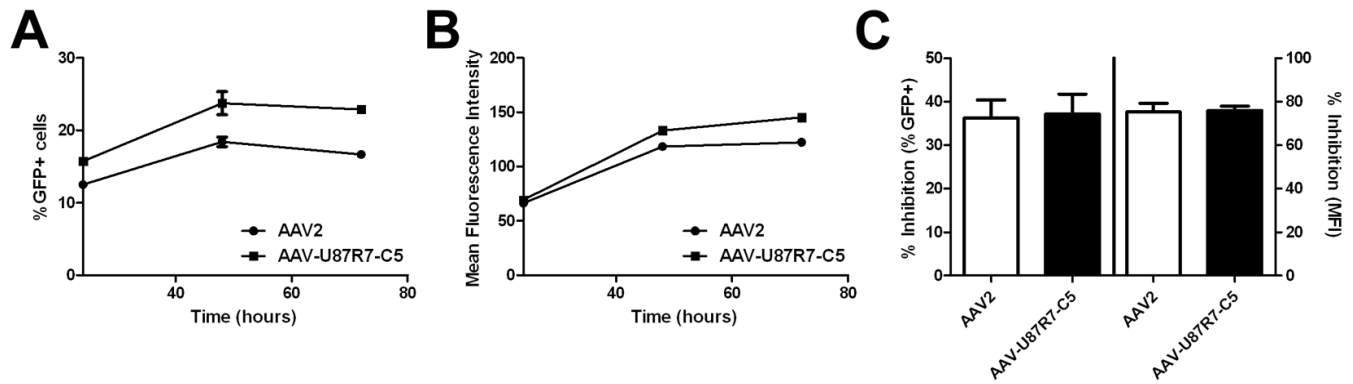


Figure 4. Characterization of U87-selected vector transduction on U87 cells

GFP expression kinetics was determined at 24, 48, 72 hours after transduction with 10^2 gc/cell of either AAV2-GFP (circles) or AAV-U87R7-C5-GFP (squares). Data is shown for **(A)** % of GFP positive cells, and **(B)** mean fluorescence intensity (MFI). **(C)** Inhibition in the percentage of GFP positive cells (left Y-axis) and MFI (right Y-axis) of AAV2 and AAV-U87R7-C5 in the presence of 100 μ g/ml of heparin. Cells were transduced with 10^4 gc/cell, and flow cytometric analysis was performed 72 hours later. Transduction in the absence of heparin was set to 100%. Error bars indicate the standard deviation from the mean.

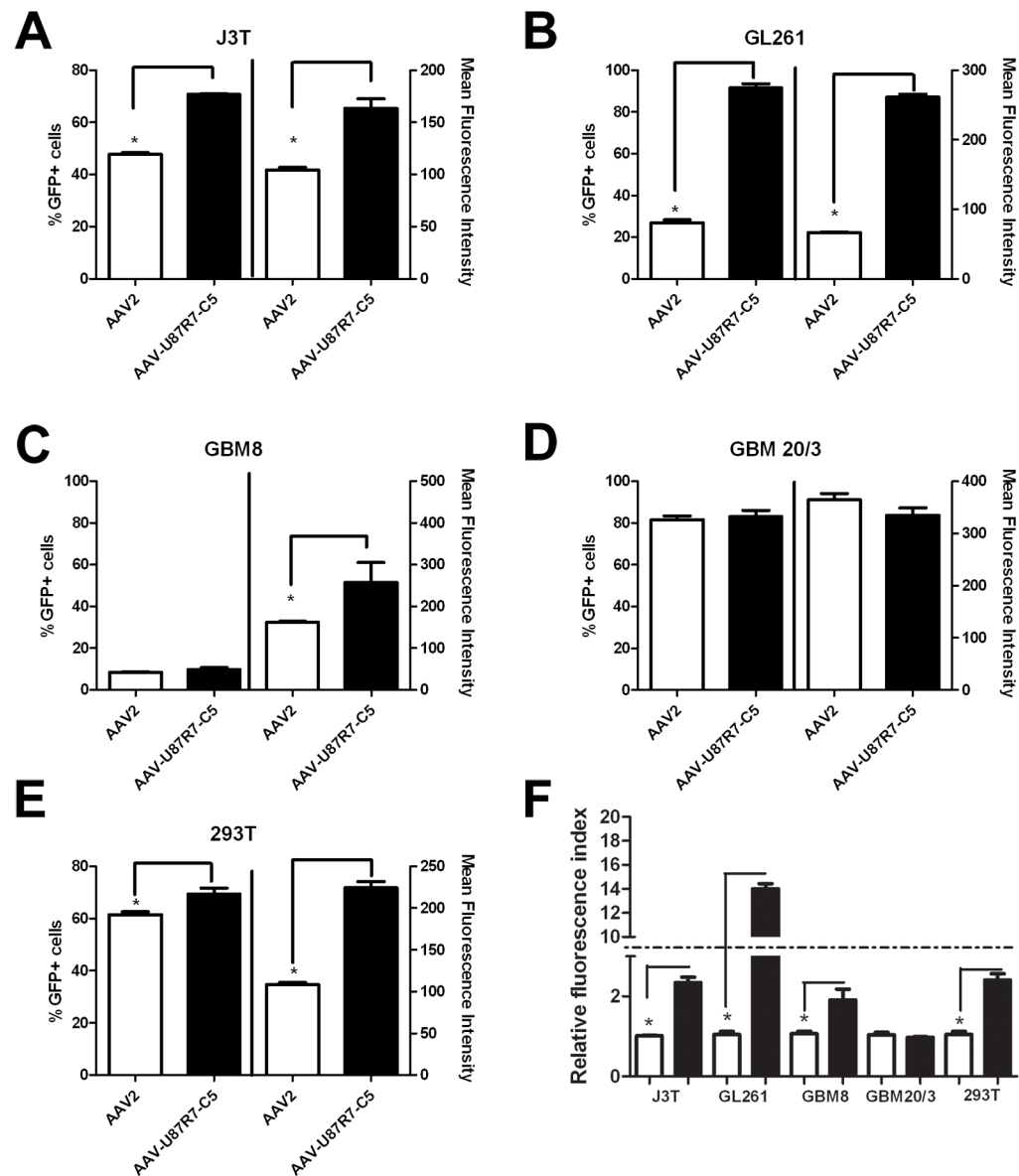


Figure 5. U87-selected vector transduction efficiency on a panel of glioma cells

Cells were transduced with 10^4 gc/cell of AAV2-GFP or AAVU87R7-C5-GFP vector. Forty-eight hours later, the percentage of GFP positive cells was determined by flow cytometric analysis. (A) J3T, dog glioma cell line; (B) GL261, mouse glioma cell line; (C) GBM8, primary human brain tumor stem cell neurospheres; (D) GBM 20/3, primary human GBM cells grown as monolayer; (E) 293T, human HEK293T cells (non-glioma cell line). (F) Relative fluorescence index of cells transduced with either AAV2-GFP (white bars) or AAV-U87R7-C5 (black bars). The fluorescence index was calculated for each sample by multiplying the percentage of GFP positive cells by the mean fluorescence intensity. For each sample in a given cell type, the fluorescence index was normalized to the lowest value in the AAV2-GFP group, which was arbitrarily set to a value of 1. Error bars indicate the standard deviation from the mean. * indicates $P < 0.05$.